Evolution of the Effective Moduli for Anisotropic Granular Materials during Pure Shear

N. Kumar, O. I. Imole, V. Magnanimo and S. Luding

Multi Scale Mechanics (MSM), Faculty of Engineering Technology, MESA+, University of Twente, P.O. Box 217, 7500 AE Enschede, The Netherlands

Abstract. We analyze the behavior of a frictionless dense granular packing sheared at constant volume. Goal is to predict the evolution of the effective moduli along the loading path. Because of the structural anisotropy that develops in the system, volumetric and deviatoric stresses and strains are cross coupled via four distinct quantities, the classical bulk and shear moduli and two anisotropy moduli. Here, by means of numerical simulation, we apply small perturbations to various equilibrium states that previously experienced different pure shear strains and investigate the effect of the microstructure (2^{nd} rank fabric tensor) on the elastic bulk response. Besides the expected dependence of the bulk modulus on the isotropic fabric, we find that both the isotropic density of contacts and the (deviatoric) orientational anisotropy affect the anisotropy moduli. Interestingly, the shear modulus of the material depends also on the actual stress state, along with the (isotropic and anisotropic) contact configuration.

Keywords: DEM, Deviatoric stress and strain, Structural Anisotropy, Calibration, PARDEM
PACS: 45.70.Cc, 81.05.Rm, 81.20.Ev

INTRODUCTION

Dense granular materials are complex systems which show unique mechanical properties different from classical fluids or solids. The behavior is highly non linear; however, for very small strain the response of a finite granular system in static equilibrium can be assumed to be linearly elastic. Understanding this effective response is important due to the large number of applications as well as for elucidating fundamental aspects of the behavior of particulate systems. However, basic features of the physics of granular elasticity are currently unsolved, like the determination of a proper set of state variables to describe the average moduli. Recent works [1, 2] show that along with the macroscopic properties (stress and volume fraction or bulk density) [1, 3], also the fabric tensor [4, 5] plays a crucial role, as it characterizes, on average, the geometric arrangement of contacts. In particular, when the material is sheared, anisotropy in the contact network develops, as related to the opening and closing of contacts, restructuring, and the creation and destruction of force-chains. This anisotropic state is at the origin of the interesting behavior of granular media during wave propagation.

Motivated by the need for a general theoretical framework for the elasticity of granular matter, we use the Discrete Element Method (DEM) [6] to study polydisperse frictionless particle assemblies . Our goal is to analyze the role of the microstructure (contact number and anisotropy) and volume fraction on the evolution of the moduli during volume conserving shear deformations.

NUMERICAL SIMULATION

We perform DEM simulations on frictionless assemblies of $N = 9261 (= 21^3)$ particles with average radius $\langle r \rangle = 1$ [mm] and density $\rho = 2000$ [kg/m^3]. For the sake of simplicity, the linear visco-elastic contact model for the normal component of the force is used [5]. Typical simulation parameters are: elastic stiffness $k = 10^8$ [kg/s^2], which determines the fastest response time scale $t_c = \pi/\sqrt{k/m} = 0.2279$ [μs] of particles with mass m; particle damping coefficient $\gamma = 1$ [kg/s]; background dissipation $\gamma_b = 0.1$ [kg/s]; and restitution coefficient $e = 0.804$ for two average sized particles. Note that the polydispersity of the system is quantified by the width $(w = r_{\max}/r_{\min} = 3)$ of a uniform size distribution [7], where $r_{\max}$ and $r_{\min}$ are the radii of the biggest and smallest particles respectively.

Averaged Quantities. From the simulations, one can determine the stress tensor $\boldsymbol{\sigma} = (1/V)\sum_{c\in V} \mathbf{l}^c \otimes \mathbf{f}^c$, i.e. the average over the contacts in the volume V of the dyadic product between the branch vector $\mathbf{l}^c$ and the contact force $\mathbf{f}^c$, where the contribution of the kinetic energy has been neglected [5, 6]. The isotropic component of the stress is the pressure $P = \mathrm{tr}(\boldsymbol{\sigma})/3$.

Besides the stress, we will focus on the fabric tensor in order to characterize the geometry/structure of the static aggregate, defined as $\mathbf{F} = (1/V)\sum_{p\in V} V^p \sum_{c\in p} \mathbf{n}^c \otimes \mathbf{n}^c$, where V^p is the particle volume for all particles p, which lie inside the averaging volume V, and $\mathbf{n}^c$ is the normal unit branch-vector pointing from the center of particle p to contact c [5]. The average isotropic fabric

Powders and Grains 2013
AIP Conf. Proc. 1542, 1238-1241 (2013); doi: 10.1063/1.4812162

is $F_v = \mathrm{tr}(\mathbf{F}) = g_3 \nu C$, where ν and C are, respectively, the volume fraction, the average number of contacts per particle (coordination number) and g_3 is a function of moments of the size distribution [7].

In addition to the isotropic components, we use the following definition to quantify the magnitude of the deviatoric parts of stress $\boldsymbol{\sigma}$ and fabric $\mathbf{F}$:

$$Q_{\mathrm{dev}} = \sqrt{\frac{(Q_1 - Q_2)^2 + (Q_2 - Q_3)^2 + (Q_3 - Q_1)^2}{2}}, \quad (1)$$

where Q_1, Q_2 and Q_3 are the eigenvalues of the tensor[4]. Finally we need to introduce as third macroscopic quantity, the strain tensor $\mathbf{E}$, i.e. the external strain field applied to the sample. Again it can be decomposed into a volumetric and deviatoric component, namely $\varepsilon_v = \mathrm{tr}(\mathbf{E})/3$ and $\varepsilon_{\mathrm{dev}}$, the latter given by Eq. (1).

Initial Isotropic preparation. The preparation consists of three parts: (i) randomization, (ii) isotropic compression, and (iii) relaxation, all equally important to achieve the initial, reference configurations. (i) First the spherical particles are randomly generated in a 3D box, with low volume fraction and rather large random velocities, such that they have sufficient space and time to exchange places and to randomize themselves. (ii) This granular gas is then isotropically compressed in order to approach a direction independent configuration, to a target volume fraction $\nu_0 = 0.640$, slightly below the jamming volume fraction $\nu_c \approx 0.665$, i.e. the transition point from fluid-like behavior to solid-like behavior [8]. (iii) This is followed by a relaxation period at constant volume fraction to allow the particles to dissipate their kinetic energy and to achieve a static configuration in mechanical equilibrium. Starting from ν_0, further isotropic compression is performed to $\nu_{\max} = 0.820$ [6] and decompression back to ν_0 and four different isotropic initial configurations from the decompression branch are realized at volume fractions $\nu_i = 0.706$, 0.751, 0.800 and 0.812.

Volume conserving deviatoric deformation. From each configuration ν_i, the system is deformed following a volume conserving deviatoric path (pure shear) with diagonal strain rate tensor $\dot{\mathbf{E}} = \dot{\varepsilon}_{\mathrm{dev}}(1, 0, -1)$, where $\dot{\varepsilon}_{\mathrm{dev}}$ (compression < 0) is the amplitude applied. In this shear deformation mode, two walls are moving in opposite directions, while the third wall is stationary [6]. During pure shear deformation, the volumetric components of stress, P, and fabric, F_v, after a tiny initial variation, saturate at steady state values, increasing with volume fraction (data not shown, see [6] for further details).

[4] Checking the magnitude of the off-diagonal components in Cartesian triaxial box, one observes that they are negligible compared to the diagonal components. Thus the diagonal components coincide (almost) with the eigen-values of the system, and we use them in Eq. (1).

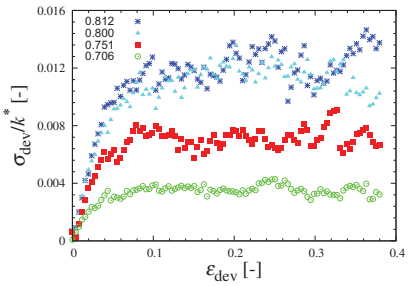

FIGURE 1. Evolution of normalized shear stress $\sigma_{\mathrm{dev}}/k^*$ versus shear strain $\varepsilon_{\mathrm{dev}}$ for the pure shear deformation for four different volume fractions, ν_i, given in the inset.

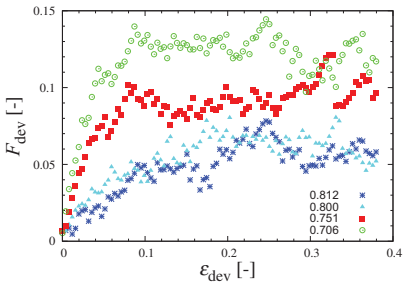

FIGURE 2. Evolution of deviatoric fabric F_{dev} versus shear strain $\varepsilon_{\mathrm{dev}}$ from data in Fig. 1.

In the following, we will analyze the evolution of the deviatoric quantities when the material is sheared. We point out here that the deviatoric stress (and the effective moduli in the next section) are normalized with $k^* = k/(2\langle r \rangle)$ in order to scale out the dependence on the particle stiffness and radius. The normalized shear stress $\sigma_{\mathrm{dev}}/k^*$ as function of the deviatoric strain, is shown in Fig. 1. The stress grows initially with applied strain until an asymptote is reached, where it remains fairly constant. The initial slope and the maximum value of stress response both increase with volume fraction ν_i. In Fig. 2, we plot the deviatoric fabric F_{dev} as a function of the deviatoric strain. For each initial volume fraction ν_i, F_{dev} builds up from small initial values (since the initial configuration is almost but not perfectly isotropic) and reaches different maximum saturation values. Note that both the slope and the steady state values of F_{dev} decrease with ν_i, showing an opposite trend of fabric than stress. The higher the volume fraction, the more isotropic the material stays during shear - which is reasonable, since in a very dense system, the particles can hardly redistribute contacts during shear.

Effective moduli. In a general framework, we can describe the constitutive behavior of an anisotropic material incrementally as

$$\begin{bmatrix} \delta P \\ \delta \sigma_{\rm dev} \end{bmatrix} = \begin{bmatrix} B & A_1 \\ A_2 & G^{oct} \end{bmatrix} \begin{bmatrix} 3\delta\varepsilon_{\rm v} \\ \delta\varepsilon_{\rm dev} \end{bmatrix}, \qquad (2)$$

where isotropic and deviatoric components of stress have been isolated and are expressed as functions of $\varepsilon_{\rm v}$ and $\varepsilon_{\rm dev}$. B is the classical bulk modulus, G^{oct}, the octahedral shear modulus, while the anisotropy moduli A_1 and A_2 provide a cross coupling between the two types of stress and strain in the model. Note that the symmetry of the stiffness matrix, related to the assumption of hyperplasticity, has been neglected here and a more general model has been considered, where thermodynamic constraint must be considered [9] to capture the inelastic nature of the materials, in the spirit of [10, 11, 12]. From Eq. (2), we can obtain all the different moduli present in the model by applying an incremental (pure volumetric or pure deviatoric) strain to the sample and measuring the incremental (volumetric or deviatoric) stress response after sufficient relaxation to achieve mechanical equilibrium [13]:

$$B = \left.\frac{\delta P}{3\delta\varepsilon_{\rm v}}\right|_{\delta\varepsilon_{\rm dev}=0}, \quad A_1 = \left.\frac{\delta P}{\delta\varepsilon_{\rm dev}}\right|_{\delta\varepsilon_{\rm v}=0}, \qquad (3)$$
$$A_2 = \left.\frac{\delta\sigma_{\rm dev}}{3\delta\varepsilon_{\rm v}}\right|_{\delta\varepsilon_{\rm dev}=0}, \quad G = \left.\frac{\delta\sigma_{\rm dev}}{\delta\varepsilon_{\rm dev}}\right|_{\delta\varepsilon_{\rm v}=0}.$$

To study the evolution of the effective moduli during shear, we perform many small strain experiments along the shear path in Figs. 1 and 2, by applying strain perturbations to the system in different anisotropic states. Since the numerical probe experiments are conducted with zero friction, we are measuring the moduli of the frictionless material, where only normal forces are involved.

RESULTS (MODULI)

Using the four packings at different ν_i, we want to determine which parameters affect the incremental response of the aggregate during the deviatoric shear path. We focus on the role of the microstructure, i.e. the fabric tensor **F**, as split in its volumetric and deviatoric components.

Bulk modulus B. In Fig. 3, we plot the variation of the normalized bulk modulus B/k^*, with the isotropic fabric $F_{\rm v}$ for packings with different volume fractions ν_i. As expected B is a purely volumetric quantity and varies with changes in the isotropic contact network, while the contact orientation anisotropy $F_{\rm dev}$ does not affect it. The bulk modulus increases systematically when the four different reference configuration are compared, and it is related to the value of $F_{\rm v}$ at a given ν_i. On the other hand, even though $F_{\rm dev}$ (see Fig. 2) changes a lot, the volumetric fabric only slightly changes during the (volume conserving) deviatoric deformation and B stays almost constant. The numerical data show good agreement with the theoretical prediction presented in [7] and reported in Fig. 3, including the second order terms therein.

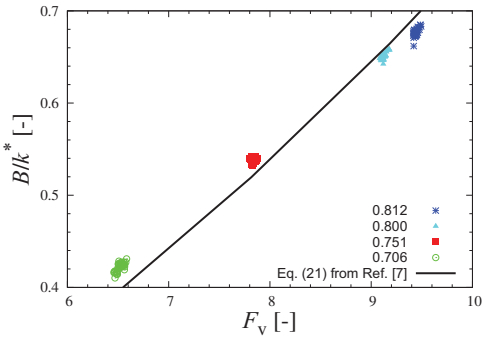

FIGURE 3. Evolution of the normalized bulk modulus B/k^* with isotropic fabric $F_{\rm v}$ during the volume conserving shear test for different volume fractions ν_i as given in the inset.

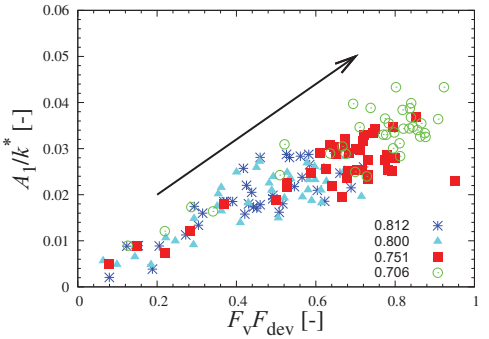

FIGURE 4. Evolution of the normalized first anisotropic modulus A_1/k^* with fabric product $F_{\rm v}F_{\rm dev}$ during the volume conserving shear test for different volume fractions ν_i as given in the inset. The arrow indicates the increasing trend during deviatoric deformation within each data-set.

Anisotropy moduli A_1 and A_2. Both A_1 and A_2 are related inherently to both deviatoric and isotropic fabric, as the whole contact network determines how the system will react to a further perturbation. In Figs. 4 and 5, the two anisotropy moduli are plotted versus the product $F_{\rm v}F_{\rm dev}$: besides their fluctuations, the data collapse on a unique curve irrespective of volume fraction and pressure. An increasing trend of both A_1/k^* and A_2/k^* with the fabric factor shows up. As the deviatoric fabric decreases with volume fraction (see Fig. 2), this leads to lower values of the moduli for denser systems. Packings

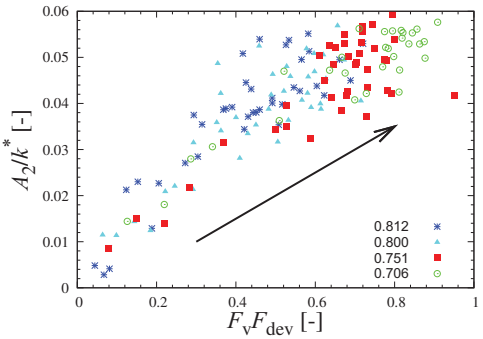

FIGURE 5. Evolution of the normalized second anisotropic modulus A_2/k^* with fabric product $F_v F_{dev}$ as in Fig. 4.

with $\nu_i = 0.800$ and $\nu_i = 0.812$ behave in a very similar fashion, in agreement with the collapse of the curves of deviatoric fabric in Fig. 2. Note that A_2/k^* is $\sim 20-30\%$ greater than A_1/k^*. This tells us that two anisotropy moduli are needed to characterize the constitutive behavior of a three dimensional granular system in contrast to the single modulus A, which was proposed for 2D [11, 12]. A deeper understanding of the phenomena that lead to a non-symmetric stiffness matrix are beyond the scope of this work and will be studied elsewhere [14].

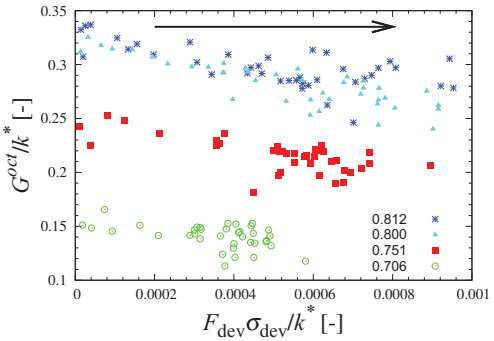

FIGURE 6. Evolution of the normalized octahedral shear modulus G^{oct}/k^* with normalized deviatoric stress and fabric product $F_{dev}\sigma_{dev}/k^*$ as in Fig. 4.

Octahedral shear modulus G^{oct}. In Fig. 6, we show the dependence of the octahedral shear modulus on $F_{dev}\sigma_{dev}$. In this case, a mixed term is needed to scale the modulus, as both the stress state and the fabric state seem to determine the incremental (pure) shear response of the material. An extra term, proportional to F_v^2, must be included to capture the value of G^{oct} in its initial isotropic state, characterized by the isotropic contact network, that stays unchanged during further deviatoric deformation, which makes $G^{oct} = \alpha F_v^2 + \beta F_{dev}\sigma_{dev}$, with constant α and β parameters (work in progress [14]).

CONCLUSION

In a triaxial cell, the four effective moduli that characterize an anisotropic granular material are inferred by performing small strain (purely volumetric and deviatoric) perturbations along the volume conserving shear path, where different anisotropic states are realized. A connection between the macroscopic elastic response and the micromechanics is established, by considering the fabric tensor. While the bulk modulus only depends on the isotropic contact network, the volumetric and deviatoric components of the fabric tensor are the fundamental state variables needed to properly model the (cross-coupling) anisotropic response. When the shear resistance is considered, both the contact network and the stress state determine the incremental behavior of the assembly. The pre-factors needed to calibrate the moduli with respect to physical experiments are subject of an ongoing study. The final goal is a (predictive) constitutive model to describe the behavior of a granular assembly in terms of a unique set of state variables.

ACKNOWLEDGMENTS

We acknowledge helpful discussions with M. B. Wojtkowski and J. Ooi. This work is financially supported by the EU funded Marie Curie Initial Training Network, FP7 (ITN-238577), PARDEM (`www.pardem.eu`).

REFERENCES

1. Y. Khidas, and X. Jia, *Phys. Rev. E* **85**, 051302:1–6 (2012).
2. L. L. Ragione, and V. Magnanimo, *Phys. Rev. E* **85**, 031304:1–8 (2012).
3. A. Ezaoui, and H. D. Benedetto, *Géotechnique* **59**, 621–635 (2009), ISSN 0016-8505.
4. M. Oda, *Soils and Foundation* **1**, 17–36 (1972).
5. S. Luding, *Journal of Physics: Condensed Matter* **17**, S2623–S2640 (2005).
6. O. I. Imole, N. Kumar, V. Magnanimo, and S. Luding, *KONA Powder and Particle Journal* **30**, 84–108 (2013).
7. F. Göncü, O. Duran, and S. Luding, *C. R. Mécanique* **338**, 570–586 (2010).
8. C. S. O'Hern, S. A. Langer, A. J. Liu, and S. R. Nagel, *Phys. Rev. Lett.* **88**, 075507:1–4 (2002).
9. I. Einav, *Int. J. Solids Struct.* **49**, 1305–1315 (2012).
10. D. Kolymbas, *Arch. Appl. Mech.* **61**, 143–154 (1991).
11. S. Luding, and E. S. Perdahcıoğlu, *Chemie Ingenieur Technik* **83**, 672–688 (2011).
12. V. Magnanimo, and S. Luding, *Granular Matter* **13**, 225–232 (2011).
13. V. Magnanimo, L. L. Ragione, J. T. Jenkins, P. Wang, and H. A. Makse, *Europhysics Letters* **81**, 34006:1–6 (2008).
14. N. Kumar, O. I. Imole, V. Magnanimo, and S. Luding, *In preparation* (2013).